Session 5: Secular evolution and internal processes: Mechanisms for fueling star formation and AGN

https://doi.org/10.1017/S1743921320004251 Published online by Cambridge University Press

https://doi.org/10.1017/S1743921320004251 Published online by Cambridge University Press

Galaxy Evolution and Feedback across Different Environments
Proceedings IAU Symposium No. 359, 2020
T. Storchi-Bergmann, W. Forman, R. Overzier & R. Riffel, eds.
doi:10.1017/S1743921320004251

INVITED LECTURE

Nature of inflows and outflows in AGNs

Keiichi Wada[1], **Yuki Kudoh**[1,3], **Naomichi Yutani**[1]
and Nozomu Kawakatu[2]

[1]Kagoshima University, Kagoshima 890-0065, Korimoto 1-21-35, Kagoshima, Japan
email: wada@astrophysics.jp

[2]National Institute of Technology, Kure Collge, Kure, Japan

[3]National Astronomical Observatory of Japan, Mitaka, Japan

Abstract. Despite many theoretical studies and observations, we still do not fully understand the feeding mechanism in AGNs even in nearby galaxies, and how feedback from AGNs affects the gas dynamics itself in the galactic central regions. In this article, we summarize our recent theoretical studies and preliminary results in terms of the mass inflow and outflows on sub-parsec to 100 parsecs scales around AGNs. We introduce different studies: 1) How do galaxy-galaxy mergers trigger AGN activity and obscuration?, 2) How do the radiative feedback affect formation of outflows and obscuration of the nucleus? and 3) How does the AGN plus starburst feedback contribute to the obscuration?

Keywords. merger, obscuration, feedback

---

1. Introduction

Nuclear activity in galaxies, such as the Active Galactic Nuclei (AGNs) and the nuclear starburst are believed to be triggered by mass inflow to the galactic central region. The underlying physics here is clear: transfer or redistribution of the angular momentum of the interstellar medium. This "mass transfer-induced activity" in galaxies has been a long-standing problem for more than three decades (e.g., Shlosman (1993)), yet not fully understood. This is partly because the fueling and feedback of AGNs span spatially many orders of magnitude. An important open question is how the energy, momentum and radiative feedback from the AGNs and the mass transfer to the central region coexist. Strong feedback may prevent from accreting the material, but if this is the case, AGN activity eventually die. The non-spherical mass accretion and outflows driven by the radiation from the accretion disc could be a key mechanism (e.g. Wada 2012, 2015, 2016, 2018a,b; see also Williamson in this volume), but episodic mass accretion and feedback during the AGN lifetime may also explain the coexistence.

Gas supply to the central 100 pc from the galactic scale would not be a big problem. As many numerical simulations have revealed, the stellar bars, galaxy-galaxy encounters or major/minor mergers may remove the angular momentum of the gas. However, the gas dynamics from several tens parsecs to the accretion disc scale is barely understood. Observationally, the structures and dynamics of the gas in the central tens of parsecs of external galaxies were not well mapped and sampled, but thanks to the ALMA, spatial structures and dynamics of the molecular gas in the central regions in some nearby AGNs have been recently resolved (Combes *et al.* (2019); Izumi *et al.* (2018); see also Garcia-Burillo in this volume). The X-ray observations may also reveal the structures of the ISM in the vicinity of the AGN. For example, Buchner *et al.* (2015) analyzed X-ray selected

© The Author(s), 2021. Published by Cambridge University Press on behalf of International Astronomical Union

https://doi.org/10.1017/S1743921320004251 Published online by Cambridge University Press

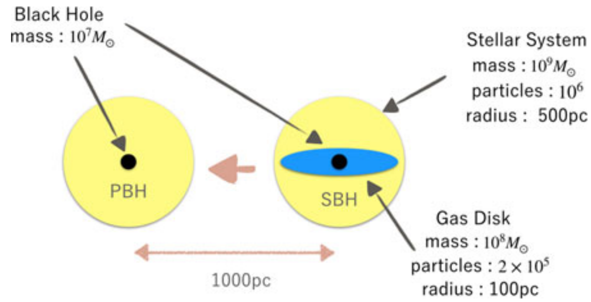

Figure 1. Schematic picture of initial setup of the fiducial model.

2000 AGNs, and they found that a large fraction of the AGNs is obscured by dense gas with $N_H > 10^{22}$ cm^{-2}. This obscured nature of AGNs should also be related with the fueling and feedback processes in the region of $r \sim$ sub-pc to several 100 pc.

In this article, we summarize our recent theoretical studies on the mass inflow and outflows from three different points of view: 1) How do galaxy-galaxy mergers trigger AGN activity and obscuration (Kawaguchi *et al.* (2020); Yutani & Wada in prep.), 2) How do the radiative feedback affect formation of outflows and obscuration of the nucleus? (Kudoh & Wada in prep.), and 3) How does the AGN plus starburst feedback contribute to the obscuration? (Kawakatu *et al.* (2020)).

2. Triggering AGN activity and obscuration during mergers

It is widely believed that galaxy mergers contribute to the growth of supermassive black holes (SMBH) in galaxies, and nuclear activity can be triggered by major mergers. Mergers of two or more nucleated galaxies result in the formation of binary BHs. Governato *et al.* (1994) studied the orbital decay of binary black holes (BBH) during galaxy mergers using N-body experiments. It has also been observed that the interstellar medium (ISM) around binary BHs may affect the orbital decay of BBHs. Because of the interaction between BBHs and the ISM, a nuclear starburst could be enhanced (Taniguchi & Wada (1996)). More recently, Prieto *et al.* (2017) studied mass transport in high-z galaxies and BH growth using cosmological hydrodynamic simulations.

In Kawaguchi *et al.* (2020), we studied the interactions between a BBH (and triple BHs) and the interstellar medium in the central sub-kpc region, using the N-body/SPH code ASURA (Saitoh *et al.* (2008, 2009); Saitoh & Makino (2013)). The numerical experiments aimed to understand the fate of the gas supplied by mergers of two or more galaxies with SMBHs, and the efficiency of the BH growth resulting from the gas supply to the galactic central region by mergers.

The model setup is schematically shown in Fig. 1. The mass resolutions are $10^3 M_\odot$ for stars and $500 M_\odot$ for gas. The gravitational softening radii are 0.5 pc for both SPH and star particles. This secondary BH (SBH) system falls toward the primary BH (PBH) system, and they merge (Fig. 2).

We found that the mass accretion rate to one SMBH exceeds the Eddington rate as the distance of two BHs rapidly decreases (see also Fig. 4). However, this rapid accretion phase does not last more than 10 Myrs, and it decreases to a sub-Eddington value (~10% of the Eddington mass accretion rate). The rapid accretion is caused by the angular momentum transfer from the gas to the stellar component, where gravitational torque dominates the torque created by the turbulent pressure gradient. The rapid accretion phase is followed by a quasi-steady accretion phase where the angular momentum is redistributed not only by the gravitational torque, but also by the turbulent viscosity in the gas disc.

https://doi.org/10.1017/S1743921320004251 Published online by Cambridge University Press

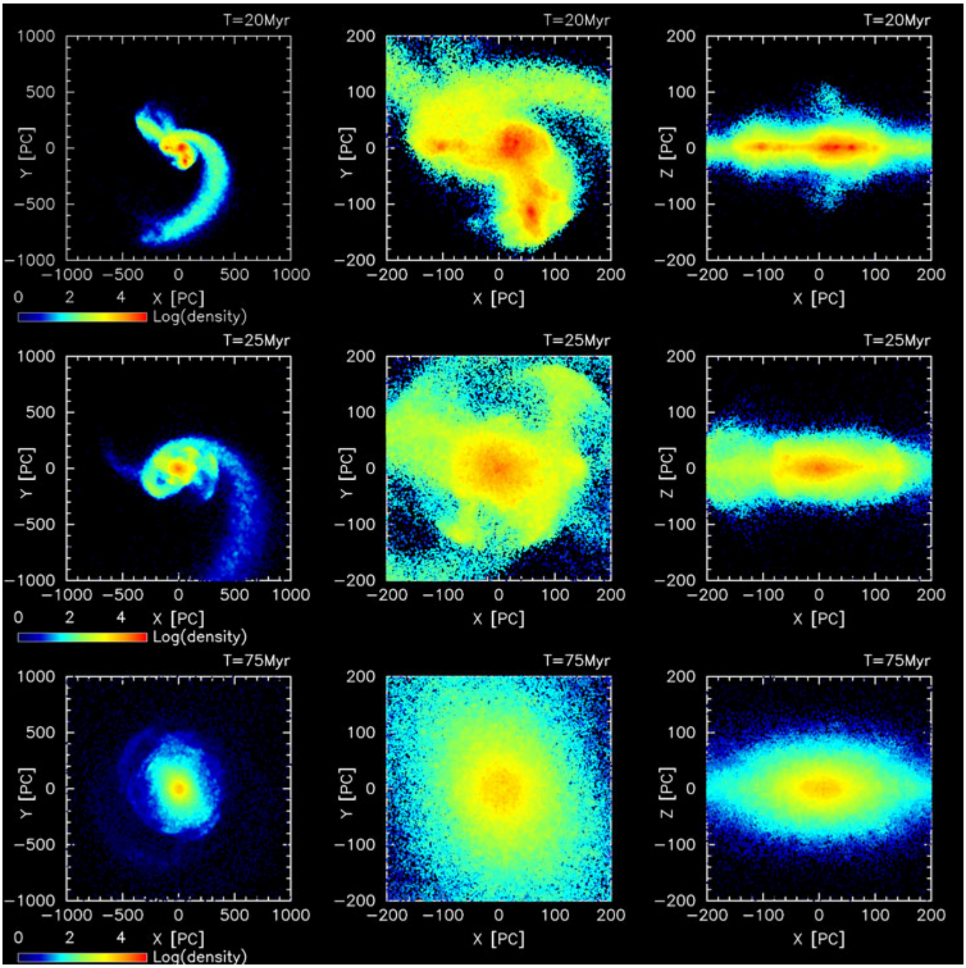

Figure 2. Evolution of gas density in the fiducial model. Three snapshots, at $t = 20, 25$, and 75 Myr, are shown. The left panels show distribution projected onto the x-y plane (2 kpc × 2 kpc), and the right two columns are close-ups for the x-y and x-z planes (0.4 kpc × 0.4 kpc). The axis units are in parsecs. The color bar represents log-scaled density ($M_\odot$ pc^{-3}).

We now examine how the energy feedback from AGNs affect the mass accretion processes. Figure 3 is a close-up of the density field in the central 200 pc × 200 pc for a model without AGN feedback and two models with AGN feedback. We found that the AGN feedback does not change the large-scale morphology (cf. Fig. 2), but it makes the gas diffuse around the BHs. In Model HighAGN, where the feedback energy rate is calculated as $0.02\dot{M}c^2$, at a mass accretion rate ($\dot{M}$) to $r = 1$ pc, almost no high-density gas remains around the BHs. This result is in contrast to Models AGN (LowAGN), where the energy conversion efficiency is 1/10 (1/100) of that in Model HighAGN.

Figure 4 (left) compares the time evolution of the mass accretion rates to SBH in the three feedback models (Models AGN, HighAGN, and LowAGN) with that of the fiducial model (hereafter, Model hP). There is no significant difference between the mass accretion rates of Model hP and Model LowAGN, and the accretion rate in Model AGN is slightly smaller than those in the other two models after $t \sim 50$ Myr. All three models show a peak of mass accretion, $\dot{M} \simeq 3$–$4 M_\odot$ yr^{-1} at approximately $t \sim 20$ Myr. However, the mass accretion rate at the peak is sub-Eddington ($0.7 M_\odot$ yr^{-1}) in model

https://doi.org/10.1017/S1743921320004251 Published online by Cambridge University Press

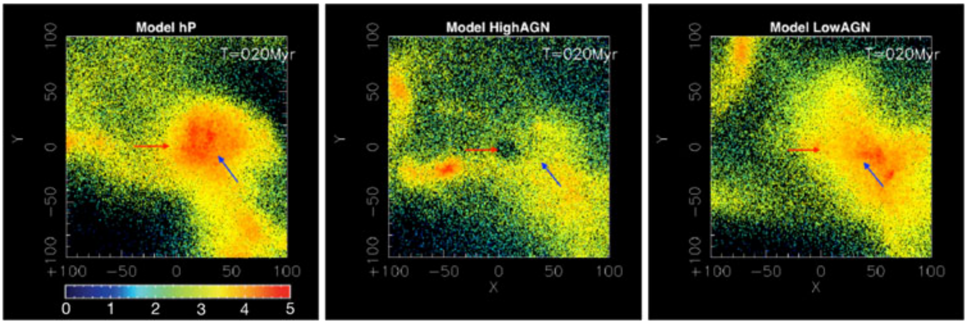

Figure 3. Gas density distributions of central 100-pc regions in Models hP (fiducial model), HighAGN, and LowAGN at $t = 20$ Myr. Positions of PBHs and SBHs are shown by red and blue arrows. The color bar represents the log-scaled gas density in $M_{\odot}$ pc^{-3}.

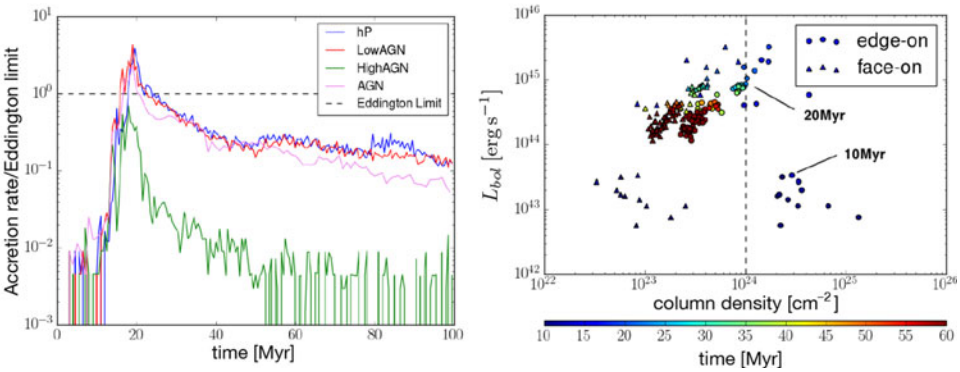

Figure 4. (left) Mass accretion rates for SBH normalized by Eddington rate for Models hP, LowAGN, HighAGN, and AGN. (right) Evolutionary track in model AGN on the plane of bolometric luminosity, based on the mass accretion to the PBH, and column densities toward the PBH.

HighAGN, and rapidly decreases to ∼1/10 in Model hP and Model LowAGN in the late accretion phase ($t > 20$ Myr). In Model HighAGN, 2% of $\dot{M}c^2$ at $r = 1$ pc is supplied to the the circumnuclear gas. This result shows that AGN feedback and black hole growth (i.e., mass accretion) can coexist in galaxy merger simulations if the feedback efficiency at 1 pc is ∼0.02−0.2%. Kawaguchi *et al.* (2020) also found that the luminous phase of the AGN ($L_{bol} > 10^{45}$ erg s^{-1}) during the merger events is heavily obscured ($N_H > 10^{24}$ cm^{-2}) by the supplied gas, and the moderate AGN feedback does not alter this property (Fig. 4(right)).

The fraction of the gas that accretes to each BH is approximately 5–7% of the supplied total gas mass ($10^8 M_{\odot}$), and 15–20% of the gas forms a circumnuclear gas within 100 pc of the BH. Star formation consumes approximately 15% of the gas supplied by mergers, and the rest forms a circumnuclear gas. Only 1/10 of the supplied gas accumulates to the central 1 pc and it is used to grow the BHs in each event. This idealized situation implies that frequent mergers are necessary for the continuous growth of BHs.

The gas inside $r < 100$ pc mostly contributes to the large column density. Ricci *et al.* (2017a) have studied 52 galactic nuclei in infrared-selected local Luminous and Ultra-luminous infrared galaxies (ULIRG) in different merger stages in the hard X-ray band, and found that the fraction of Compton-thick AGN in late merger galaxies are higher than in local hard X-ray selected AGN. They suggested that the material is most effectively

https://doi.org/10.1017/S1743921320004251 Published online by Cambridge University Press

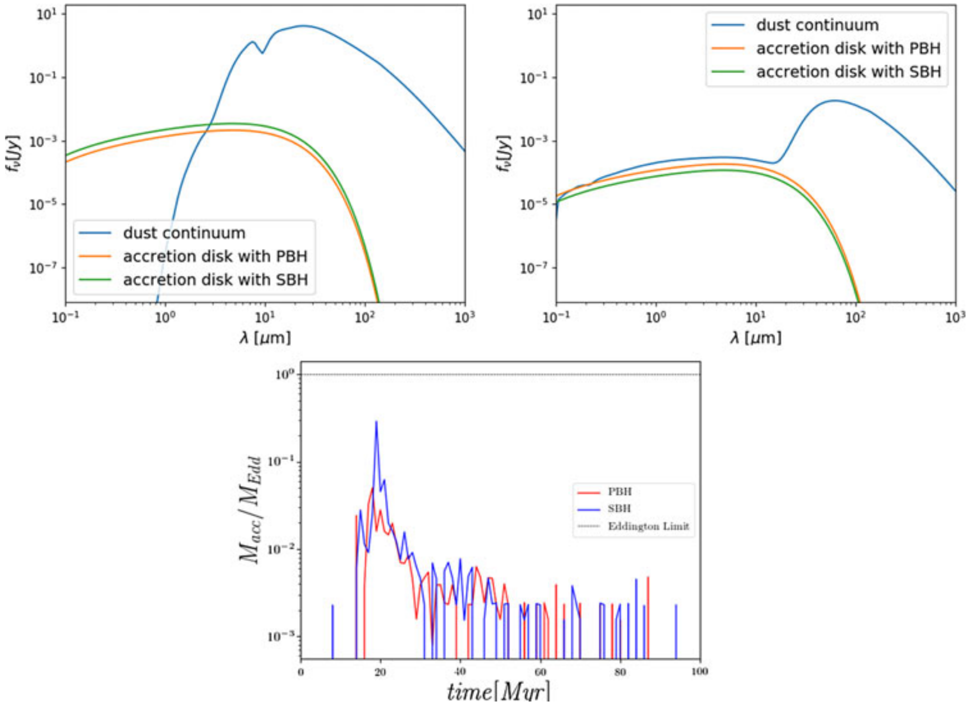

Figure 5. SED evolution of mergers with $M_{BH} = 10^7 M_\odot$, $M_{gas} = 2 \times 10^8 M_\odot$ and $M_{star} = 1 \times 10^9 M_\odot$, $R_{gas} = 100$ pc. Top left is at $t = 20$ Myr and top right is at $t = 70$ Myr. The distance of the observer is 100 Mpc. The bottom panel shows time evolution of the mass accretion rate. When two systems are merged ($t \sim 20$ Myr), the accretion rates become the maximum value $\sim$0.3 for PBH and 0.06 of the Eddington rate. The mass resolution is 1000 $M_\odot$ for both gas and stars. (Yutani, & Wada in prep.)

funnelled to the inner tens of parsecs during the late stages of galaxy mergers. Our results above are qualitatively consistent with Ricci *et al.* (2017a).

Our model can also be compared with the recent findings of a high fraction of Compton-thick AGNs in merging systems and AGNs in dust-obscured galaxies (DOGs) (Dey *et al.* (2008); Fiore *et al.* (2008); Toba *et al.* (2017); Riguccini *et al.* (2019)). In Fig. 5, we show preliminary results of the SED evolution during the mergers of two gas-rich systems with BHs, which is slightly different from the model set-up in Kawaguchi *et al.* (2020). Here the AGN feedback efficiency is assumed to be 0.2%. At $t = 20$ Myr, when the mass accretion rate to the PBH and SBH is 30% of the Eddington rate, the UV light from the nucleus is attenuated. At $t \sim 70$ Myr after the two systems are merged, the nucleus becomes "bluer" and less obscured (Fig. 5, top right).

3. How does the radiative feedback affect outflows formation and obscuration?

Using a systematic multi-wavelength survey of hard X-ray-selected black holes, Ricci *et al.* (2017b) suggested that radiation pressure on dusty gas is the main physical mechanism regulating the distribution of the circumnuclear material. We are trying to confirm this observational result by using a grid-based MHD code, CANS+ (Matsumoto *et al.* (2019)). Figure 6 shows a preliminary result, where density and temperature distributions of three models with the Eddington ratios of 0.01, 0.1 and 1.0 in the central 16 pc are shown. The model is axisymmetric, and the grid cell size is 0.01 pc. The black hole mass is $10^7 M_\odot$. The non-spherical radiation feedback (the radiation pressure for dust

https://doi.org/10.1017/S1743921320004251 Published online by Cambridge University Press

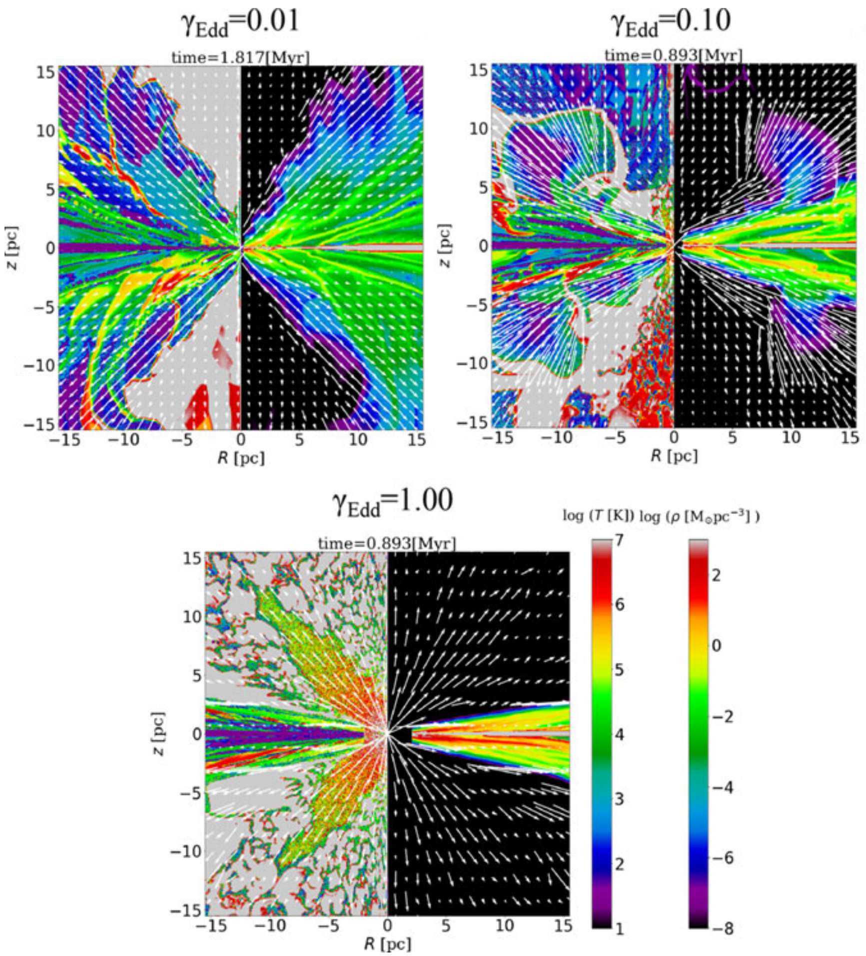

Figure 6. The dependence of the outflow properties around AGN on the Eddington ratio (γ_{Edd}). Density (right panels) and temperature (left panels) are shown (Kudoh, & Wada in prep.)

and the X-ray heating) is considered. As suggested by the observations, the scale height of the disc becomes smaller for larger the Eddington ratio. However, for much smaller γ_{Edd}, the radiation-driven outflows themselves are not formed; therefore it is difficult to explain the high obscured fraction in AGNs with $\gamma_{Edd} \ll 0.01$ only by the circumnuclear region on this scale.

4. How do the AGN and starburst feedback contribute to obscuration?

In Kawakatu *et al.* (2020), we investigated the structure at 10 pc scale obscuring the circumnuclear discs (CNDs) by considering the SN feedbacks from nuclear starburst and the effect of anisotropic radiation pressure. We explored how structures of 1–10 pc dusty CNDs depend on the BH mass ($M_{\rm BH}$), AGN luminosity ($L_{\rm AGN}$), and physical properties of CNDs. The model is based on Wada & Norman (2002); Kawakatu & Wada (2008), and Kawakatu & Wada (2009).

https://doi.org/10.1017/S1743921320004251 Published online by Cambridge University Press

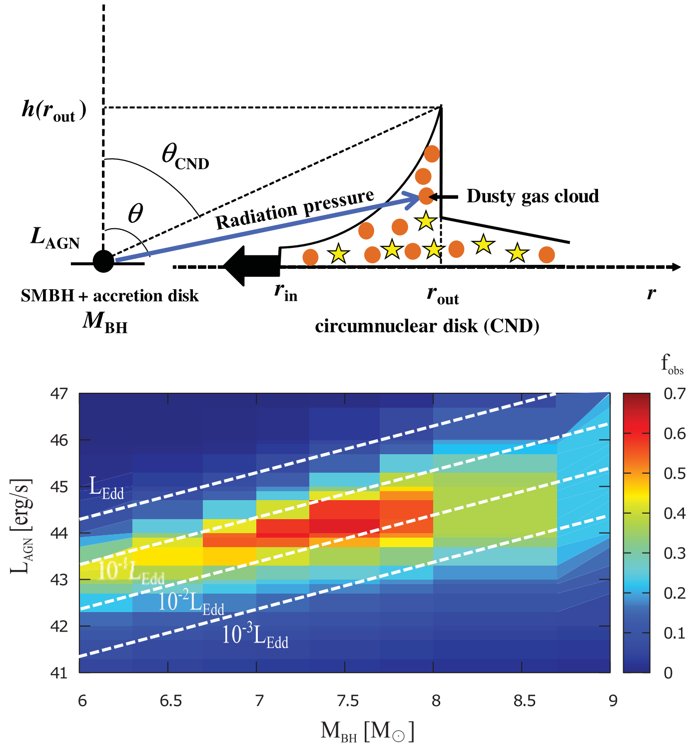

Figure 7. (top) A schematic picture of the CND with nuclear starbust irradiated by the radiation from the accretion disc. (bottom) Obscured fractions as a function of the AGN luminosity and the black hole mass.

4.1. *Structure of circumnuclear discs with the radiative feedback from the AGN*

We assume that the vertical structure of CNDs is in hydrostatic equilibrium (see details in Wada & Norman 2002). We suppose that the turbulent pressure associated with SN explosions is balanced with gravitation in the vertical direction, i.e.,

$$\rho_{\rm g} v_{\rm t}^2 = \rho_{\rm g} g h, \tag{4.1}$$

where $\rho_{\rm g}$, $v_{\rm t}$, and h are the gas density, turbulent velocity, and scale height of the disc, respectively. Under the energy between supernova feedback $E_{\rm in}$ and the turbulent dissipation $E_{\rm out}$, the turbulent velocity $v_{\rm t}$ and scale height h are expressed as

$$v_{\rm t} = \left(\frac{GM_{\rm BH}}{r^3}\right)^{1/2} h, \tag{4.2}$$

$$h = \left(\frac{GM_{\rm BH}}{r^3}\right)^{-3/4} (\eta E_{\rm SN} C_*)^{1/2},$$
$$= 14\,{\rm pc} \left(\frac{C_*}{10^{-8}\,{\rm yr}^{-1}}\right)^{1/2} \left(\frac{M_{\rm BH}}{10^7 M_\odot}\right)^{-3/4} \left(\frac{r}{30\,{\rm pc}}\right)^{9/4}. \tag{4.3}$$

Here C_* is the star-formation efficiency and E_{SN} is the ejecta energy of a single supernova. The model predicts that the disc will have a concave structure due to the SN-driven turbulence, i.e., $h \propto r^{9/4}$ (see Fig. 7 top).

https://doi.org/10.1017/S1743921320004251 Published online by Cambridge University Press

In order to examine how the radiation pressure from AGNs (i.e., accretion disc) affects the structure of CNDs predicted by the SN-driven turbulent disc (eq. 4.3), we consider anisotropic radiation from an AGN emitted by an accretion disc around an SMBH. We evaluate the obscuring fraction, $f_{\rm obs} \equiv \tan(\pi/2 - \theta_{CND})$, predicted by the model that takes into account not only the SN feedback but also the radiative feedback from the AGN.

4.2. *Summary of main results*

• The obscuring fraction, $f_{\rm obs}$, peaks at the luminosity $L_{\rm AGN,p} \sim 10\%$ of the AGN Eddington luminosity ($L_{\rm Edd}$), and the maximal value of $f_{\rm obs}$ is ~0.6 for less massive SMBHs (e.g., $M_{\rm BH} < 10^8 M_\odot$). For lower $L_{\rm AGN}$, the obscuring fraction is determined by the SN feedback, while the radiative feedback is important for higher $L_{\rm AGN}$. On the other hand, for massive SMBHs (e.g., $M_{\rm BH} > 10^8 M_\odot$), the obscuring fraction $f_{\rm obs}$ is always low (<0.2), and it is independent of $L_{\rm AGN}$ because the scale height of CNDs is mainly regulated by the maximal star-formation efficiency, $C_{*.\rm max}$, in CNDs.

• We compared the predicted obscuring fraction $f_{\rm obs}$ with mid-IR observations (Ichikawa *et al.* (2019)). The SN + radiation pressure model is consistent with the IR obscuring fraction for massive BHs with $M_{\rm BH} = 10^8 M_\odot$. This implies that an intense nuclear starburst with $C_{*,\rm max} = 10^{-7}\ {\rm yr}^{-1}$ contributes to the obscuration in these objects. In addition, our model can qualitatively explain the observed behaviour of $f_{\rm obs}$ as a function of the X-ray luminosity (e.g., Burlon *et al.* (2011)). However, $f_{\rm obs,X}$ is always greater than our theoretical predictions, especially for AGNs with low Eddington luminosity ratio ($L_{\rm AGN}/L_{\rm Edd} < 10^{-2}$).

References

Buchner, J., Georgakakis, A., Nandra, K., *et al.* 2015, *ApJ*, 802, 89
Burlon, D., Ajello, M., Greiner, J., *et al.* 2011, *ApJ*, 728, 58
Combes, F., García-Burillo, S., Audibert, A., *et al.* 2019, *A&Ap*, 623, A79
Debuhr, J., Quataert, E., & Ma, C.-P. 2011, *MNRAS*, 412, 1341
Dey, A., Soifer, B. T., Desai, V., *et al.* 2008, *ApJ*, 677, 943
Fiore, F., Grazian, A., Santini, P., *et al.* 2008, *ApJ*, 672, 94
Governato, F., Colpi, M., & Maraschi, L. 1994, *MNRAS*, 271,
Kawaguchi, T., Yutani, N., & Wada, K. 2020, *ApJ*, 890, 125
Kawakatu, N., Wada, K., & Ichikawa, K. 2020, *ApJ*, 889, 84
Kawakatu, N. & Wada, K. 2008,*ApJ*, 681, 73
Kawakatu, N. & Wada, K. 2009, *ApJ*, 706, 676
Izumi, T., Wada, K., Fukushige, R., *et al.* 2018, *ApJ*, 867, 48
Ichikawa, K., Ricci, C., Ueda, Y., *et al.* 2019, *ApJ*, 870, 31
Matsumoto, Y., *et al.* "Magnetohydrodynamic Simulation Code CANS+: Assessments and Applications", *Publ. Astron. Soc.* Japan, doi:10.1093/pasj/psz064
"Mass-transfer induced activity in galaxies", ed. by I. Shlosman, 1994, Cambridge Univ. Press, NY
Prieto, J., Escala, A., Volonteri, M., & Dubois, Y. 2017, *ApJ*, 836, 216
Ricci, C., Bauer, F. E., Treister, E., *et al.* 2017a, *MNRAS*, 468, 1273
Ricci, C., Trakhtenbrot, B., Koss, M. J., *et al.* 2017b, *Nature*, 549, 488
Riguccini, L. A., Treister, E., Menéndez-Delmestre, K., *et al.* 2019, *AJ*, 157, 233
Saitoh, T. R., Daisaka, H., Kokubo, E., *et al.* 2008, *PASJ*, 60, 667
Saitoh, T. R., Daisaka, H., Kokubo, E., *et al.* 2009, *PASJ*, 61, 481
Saitoh, T. R. & Makino, J. 2013, *ApJ*, 768, 44
Taniguchi, Y. & Wada, K. 1996, *ApJ*, 469, 581

https://doi.org/10.1017/S1743921320004251 Published online by Cambridge University Press

Toba, Y., Nagao, T., Kajisawa, M., *et al.* 2017, *ApJ*, 835, 36

Wada, K. & Norman, C. A. 2002, *ApJL*, 566, L21

Wada, K., Yonekura, K., & Nagao, T. 2018a, *ApJ*, 867, 49

Wada, K., Fukushige, R., Izumi, T., *et al.* 2018b, *ApJ*, 852, 88

Wada, K., Schartmann, M., & Meijerink, R. 2016, *ApJL*, 828, L19

Wada, K. 2015, *ApJ*, 812, 82

Wada, K. 2012, *ApJ*, 758, 66

https://doi.org/10.1017/S1743921320004251 Published online by Cambridge University Press

Hekatelyne Carpes

Sandra Raimundo

https://doi.org/10.1017/S1743921320004251 Published online by Cambridge University Press